Published in final edited form as:
Curr Biol. 2011 September 13; 21(17): 1450–1459. doi:10.1016/j.cub.2011.07.046.

Distinct roles for F-BAR proteins Cdc15p and Bzz1p in actin polymerization at sites of endocytosis in fission yeast

Rajesh Arasada[1] and **Thomas D. Pollard**[1,2,*]

[1]Department of Molecular Cellular and Developmental Biology, Yale University, PO Box 208103,New Haven, CT 06520-8103 USA

[2]Department of Molecular Biophysics and Biochemistry and of Cell Biology, Yale University, PO Box 208103,New Haven, CT 06520-8103 USA

Summary

Background—Genetic analyses of budding and fission yeast identified >50 proteins that assemble at sites of clathrin-mediated endocytosis in structures called actin patches. These proteins include clathrin, clathrin-interacting proteins, actin binding proteins and peripheral membrane proteins such as F-BAR proteins. Many questions remain regarding the interactions of these proteins, particularly the participation of F-BAR proteins in the assembly of actin filaments.

Results—Our microscopic and genetic interaction experiments on fission yeast show that F-BAR proteins Cdc15p and Bzz1p accumulate in two distinct zones on invaginating membrane tubules and interact with Myo1p and Wsp1p, nucleation-promoting factors for Arp2/3 complex. The two F-BAR proteins peak prior to movement of the actin patch and their accumulation in actin patches depends on the nucleation-promoting factors. At their peak local concentrations, we estimated the stoichiometries of the proteins in actin patches to be 1 Bzz1p per 2 Wsp1p and 1 Cdc15p per Myo1p. Purified Bzz1p has two SH3 domains that interact with Wsp1p and stimulate actin polymerization by Arp2/3 complex. Cells lacking either Cdc15p or Bzz1p assemble 3- to 5-fold less actin in patches (in spite of normal levels of Wsp1p, Myo1p and Arp2/3 complex) and patches move shorter distances from the plasma membrane.

Conclusion—We propose that during clathrin-mediated endocytosis F-BAR proteins interact with nucleation promoting factors to stimulate Arp2/3 complex in two different zones along the invaginating tubule. We further propose that polymerization of actin filaments in these two zones contributes to membrane scission.

Introduction

Cells use endocytosis to take up nutrients and internalize cell surface molecules. Yeasts rely mainly on clathrin-dependent mechanisms for endocytosis, while animal cells also use other mechanisms [1-4]. Clathrin-mediated endocytosis involves recruitment of proteins to a site where the plasma membrane invaginates and pinches off a vesicle. Fluorescence microscopy documented the time course of assembly of many of these proteins in yeast [5].

*Correspondence: thomas.pollard@yale.edu.

In mammalian cells scission of an endocytic vesicle depends on the GTPase dynamin, which accumulates at the neck of the membrane invagination [6]. Budding and fission yeast encode three dynamin homologs, but none localize in actin patches [5]. Some studies showed that the budding yeast dynamin homolog Vps1p interacts with Sla1p and that *Δvps1* mutants accumulate depolarized actin aggregates and fail to internalize membrane receptors [7, 8]. Other studies reported that deletion of Vps1p did not affect endocytosis or the ultrastructure of actin patches in budding yeast [5, 9] or fission yeast [10].

Both yeasts depend on actin polymerization to generate tubular invaginations of the plasma membrane at sites of endocytosis [9]. Actin assembly is also important in clathrin-dependent, caveolin-dependent and clathrin/caveolin-independent endocytosis in animal cells [1, 11-15]. Mammalian cells use the same proteins to make both small clathrin coated pits independent of the actin cytoskeleton and larger clathrin coated plaques that require actin cytoskeleton [16]. In all carefully studied systems actin assembly during endocytosis depends on Arp2/3 complex and its nucleation promoting factors [5, 13, 17-20].

Some early endocytic proteins such as Pan1, Sla2, Hip1, Hip1R, proteins of the BAR superfamily (amphiphysin, SNX9, Toca1, Cip4 and FBP17) and dynamin associate with both membrane lipids and components of the actin cytoskeleton. These interactions link the plasma membrane and the actin cytoskeleton [6, 21-23], but the connections between actin polymerization and membrane reorganization are less well understood than actin assembly.

We used quantitative fluorescence microscopy to study the roles of F-BAR proteins Bzz1p and Cdc15p during endocytosis in fission yeast. Mutations in the *bzz1*$^+$ gene or depletion of Cdc15p impaired endocytosis and assembly of actin filaments in patches in spite of normal accumulation of WASp (Wsp1p), myosin-I (Myo1p) and Arp2/3 complex. Cdc15p assembled stoichiometrically with Myo1p, while Bzz1p assembled stoichiometrically with and activated Wsp1p. These features as well as genetic interactions lead us to propose that these two F-BAR proteins set up separate zones of actin assembly on tubular necks connecting coated pits to the surface membrane.

Results

F-BAR Proteins of *S. pombe*

The *S. pombe* genome contains seven genes encoding F-BAR domains (Figure S1), a domain highly conserved from amoebas to mammals in the “pombe Cdc15 homology” (PCH) family of proteins. Previous work characterized six *S. pombe* F-BAR proteins, Cdc15p [24], Bzz1p [25], Imp2p [26], Rga7p [27-29], Rga8p [30] and Rga9p [30]. ORF SPBC12C2.05c *bzz1*$^+$ [25], groups with *Saccharomyces cerevisiae bzz1* [31] on a phylogenetic tree of F-BAR domains (Figure S1A). Uncharacterized *S. pombe* ORF SPBC4C3.06 grouped with *S. cerevisiae,* suppressor for yeast profilin 1, *syp1*, so we named SPBC4C3.06 *syp1*$^+$. Figures 1 and S1 illustrate the domain architecture of these proteins. The *cdc15*$^+$ gene is essential for viability [24], but strains with single deletions of the genes for five other F-BAR proteins were viable (Table I). We did not attempt to isolate a *Δrga9* strain.

We expressed all seven F-BAR proteins fused with a monomeric fluorescent protein from their native loci under the control of their endogenous promoters. Cdc15p was tagged on the N-terminus [32], while the monomeric fluorescent protein was fused to the C-termini of the other proteins. All of the strains depending on F-BAR proteins tagged with mNFPs were viable and grew normally (Figure S1J). Syp1p is associated with early stages of endocytosis, Cdc15p and Bzz1p are associated with actin patches and each of the other 4 F-BAR proteins had a unique temporal and spatial distribution in cells (Figures 1A, 1B and S1B - S1I; Table

I). Cdc15p is unique among these proteins, because it participates in both endocytosis and cytokinesis [24, 33] (Figures 1A and S1B). Similar to *S. cerevisiae* Bzz1p, *S. pombe* Bzz1p-mNFP concentrated in punctate structures at the tips of cells that we confirmed to be actin patches by colocalization of Bzz1p-mEGFP with the actin patch markers fimbrin or coronin tagged with mCherry (Figure 1B, data not shown).

Our study focused on actin patches, so we tested if mEGFP tagged Cdc15p and Bzz1p were functional by crossing these strains with mutants that exhibit synthetic interaction phenotypes when combined with mutations of the *cdc15*$^{+}$ or *bzz1*$^{+}$ genes (Table II and see below). The mEGFP-Cdc15p fusion protein was functional as a genetic cross between *mEGFP-cdc15* and a *Δwsp1* strain produced viable *Δwsp1* cells expressing mEGFP-Cdc15p. mEGFP-Cdc15p localized to actin patches and contractile rings in *Δwsp1* cells (Figure S1K). Our failure to generate *Δmyo1* mutant cells expressing Bzz1p-mEGFP revealed that Bzz1p-mEGFP was not fully functional, but an endocytosis assay with FM4-64 showed that cells depending on Bzz1p-mEGFP took up the fluorescent dye as well as wild type cells (Figure S1M). Bzz1p tagged on its N-terminus was less functional, since mEGFP-Bzz1p expressed from the native locus failed to localize to the actin patches (Figure S1L) and crosses with *Δmyo1* cells produced only 2 or 3 viable spores.

Time course of Cdc15p and Bzz1p assembly in actin patches

Time-lapse microscopy of live cells expressing fluorescent fusion proteins established the timing of the accumulation and disappearance of Cdc15p and Bzz1p in actin patches compared with tagged Wsp1p, Myo1p and coronin Crn1p (Figures 1C and 1D). We used the fluorescence intensity of actin patches in cells expressing single fluorescent fusion proteins to measure the numbers of molecules at 1 s time intervals [34, 35] (Figures 1C, 1D, S2E - S2H and S2M). We used two criteria to align all of the measured proteins on the same time scale: the initial movement of patches was defined as time zero; and for patch components such as Myo1p and Cdc15p that did not move, we confirmed their relative positions over time by imaging strains expressing a pair of fluorescent proteins tagged with mYFP and mCFP (Figures S2A - S2D).

Bzz1p-mEGFP and mEGFP-Cdc15p appeared in, peaked and disappeared from actin patches over ~10 s (Figures 1D, S2E and S2F). The two proteins remained together in actin patches until they reached their peak concentrations and then began to separate. Myo1p peaked at ~170 (±36; one standard deviation) molecules ~2 s earlier than Cdc15p, but their numbers were equal when Cdc15p peaked at about 130 (±27) molecules (Figures 1D, S2F and S2G). Both Cdc15p and Myo1p were stationary as their numbers declined (0.05±0.07 μm and 0.03±0.04 μm from the origin) (Figures 1C, 1E, S2J and S2K). Wsp1p peaked at ~140 (±16) molecules ~1 s before Bzz1p peaked at ~75 (±15) molecules (Figures 1C, 1D, S2H and S2E). Like Wsp1p (0.42±0.06 μm from the origin) and verprolin Vrp1p, Bzz1p moved a short distance as it dissipated (0.25±0.03 μm from the origin) (Figures 1C, 1E, S2L and S2I) [36].

Genetic interactions among activators of Arp2/3 complex

Wsp1p and Myo1p define two independent pathways of actin assembly at sites of endocytosis in vivo, with either pathway being sufficient for cell viability [36, 37]. To test genetic interactions with activators of Arp2/3 complex we used a temperature sensitive *cdc15*$^{+}$ mutant (*cdc15-127*) and a *bzz1*$^{+}$ deletion mutant with the *ura4*$^{+}$ gene replacing the entire *bzz1*$^{+}$ ORF. Cells lacking Bzz1p were shorter than wild type cells at 25°C, and grew slower than wild type cells at higher temperatures (Table II). We generated double mutant strains Δ*bzz1* Δ*wsp1*, *cdc15-127* Δ*wsp1*, and *cdc15-127* Δ*myo1*, but failed to generate Δ*bzz1* Δ*myo1,* suggesting that Δ*bzz1* is synthetically lethal with Δ*myo1* (Table II). The

cdc15-127 Δ*wsp1* strain failed to grow at temperatures greater than 25°C suggesting that *cdc15-127* is synthetically lethal with Δ*wsp1* (Table II). Both the Δ*wsp1* and Δ*myo1* strains carried a complementing plasmid to assist in these crosses.

Interactions of Bzz1p and Cdc15p with nucleation promoting factors in vivo

We isolated mutants to test the roles of Cdc15p and Bzz1p in endocytosis. The *cdc15*$^{+}$ gene is essential, so we replaced the endogenous promoter with a thiamine-repressible nmt1 promoter [41×] to allow thiamine to repress the level of Cdc15p 50-fold from 12 μM to 0.2 μM in wild type cells (Figure S3A).

An endocytosis assay showed that both Bzz1p and Cdc15p are required for normal uptake of a lipophilic dye FM4-64 (Figure 2A). We used a pulse chase design, where a cold temperature blocked endocytosis while the plasma membrane was labeled by exposing cells to 20 μM FM4-64 dye for 15 min. Raising the temperature to 25°C on the microscope stage reinitiated endocytosis, which we followed over time by fluorescence microscopy. Mutant Δ*bzz1* and *41xnmt1cdc15* cells took up FM4-64 much slower than wild type cells: by 15 min 85% of wild type cells but none of the Δ*bzz1* cells and only 15% of *41xnmt1cdc15* cells concentrated the dye in the vacuolar membranes (Figure 2A and 2B).

Cells lacking Bzz1p or depleted of Cdc15p had serious defects in actin patch movement (Figure 2C) even though these patches contained normal amounts of Myo1p, Wsp1p and Arp2/3 complex (Figures 2I – 2K and S3G – S3O). In wild type cells actin patches marked with coronin Crn1p-mEGFP moved persistently away from the plasma membrane (Figures 2C, 2D and S3B), while coronin moved only ~300 nm in cells lacking Bzz1p or depleted of Cdc15p (Figures 2C, S3C and S3D) or lacking Wsp1p or Myo1p (Figures 2C, 2G, 2H, and S3E, S3F). Furthermore 38% of patches in *Δbzz1* cells (n = 24 patches) and 19% of patches in *41xnmt1cdc15* cells (n = 32 patches) stalled or retracted back to the plasma membrane after moving a short distance (Figures 2E and 2F).

Actin patches in cells without Bzz1p or depleted of Cdc15p assembled only 20-33% as much GFP-actin as in wild type cells (Figures 2L, S3P– S3R). GFP-tagged actin cannot replace native actin in fission yeast [34, 38], so we expressed GFP-actin from the *leu*$^{+}$ locus in the genome under the control of an *nmt1* promoter (medium strength *41xnmt1* promoter in Δ*bzz1* cells and a strong *3xnmt1* promoter in *41xnmt1cdc15* cells). Thiamine repressed Cdc15p expression in *41xnmt1cdc15* cells, as evident from the phenotype, but the *3xnmt1* promoter allowed the cells to express about the same levels of GFP-actin in wild type cells (3.6 μM, 11% of total actin), Δ*bzz1* cells (3.2 μM, 10.3% of total actin) and *41xnmt1cdc15* cells in thiamine (4.6 μM, 15% of total actin) (Figures S3S and S3T). Control experiments verified that expression of low levels of mNFP-actin did not alter the morphology of the cells, interfere with the formation of actin cables or contractile rings or with the dynamics of other patch components tracked with CapBp (Figures S3U and S3V).

Bzz1p SH3 domains bind Wsp1p and stimulate its nucleation promoting activity

We used domain deletion mutants to study the roles of the two Bzz1p SH3 domains in actin polymerization in cells. Bzz1p lacking one or both the SH3 domains was tagged with mYFP at the C-terminus and expressed at near wild type levels from the *bzz1*$^{+}$ locus (Figure S4A). Bzz1p lacking a single SH3 domain accumulated in actin patches, which assembled 34% less GFP-actin (268 molecules) than wild type cells (407 molecules) (Figure 3B). Bzz1pΔSH3ΔSH3 lacking both SH3 domains did not accumulate in actin patches (Figure 3A) and these patches assembled only 81 molecules of GFP-actin, similar to Δ*bzz1* cells (Figure 3B).

Equilibrium binding assays showed that both SH3 domains of Bzz1p contribute to binding *S. pombe* WASp. Purified *S. pombe* Wsp1p poly (p)-VCA (residues 129-574 including the polyproline domain and VCA) bound GST-Bzz1p-SH3SH3 with both SH3 domains with a much higher affinity (K_d ~0.1 μM) (Figure 3C) than GST-Bzz1p-SH3 with just the C-terminal SH3 domain (K_d ~2 μM) (Figure 3D). Neither GST nor GST-Cdc15p-SH3 bound Wsp1p poly (p)-VCA (data not shown).

Actin polymerization assays showed that dimers of Bzz1p-SH3 domains stimulate the ability of Wsp1p poly (p)-VCA to activate Arp2/3 complex (Figures 3E and 3F). Purified *S. pombe* Arp2/3 complex had little effect on the time course of spontaneous assembly of muscle actin even in the presence of 500 nM monomeric Wsp1p poly (p)-VCA with or without a monomeric construct consisting of the two Bzz1pSH3 (Figure 3E). On the other hand, the combination of Arp2/3 complex with monomeric Wsp1p poly (p)-VCA and dimeric GST-Bzz1pSH3 stimulated actin polymerization nearly as well as Arp2/3 complex with dimeric GST-Wsp1p poly (p)-VCA. The rate of actin polymerization reached a maximum with 1 μM GST-Bzz1pSH3 and 0.5 μM Wsp1p poly (p)-VCA (Figure 3F).

Myo1p tail is required to recruit Cdc15p to patches

Experiments with deletions from the tail of Myo1p showed that the TH2 domain is required for Cdc15p to localize in actin patches, confirming evidence from yeast two hybrid, biochemical and immunoprecipitation assays [33]. We crossed cells expressing Cdc15p-mEGFP with *Δmyo1* cells complemented with COOH-terminal deletion mutants of Myo1p known to localize to actin patches and rescue the growth and mating defects of *Δmyo1* [37]. Cdc15p-mEGFP concentrated in actin patches with similar time courses in wild type cells (8-12 s) and cells depending on Myo1p-H/1/2/3 (*myo1ΔA*, lacking the C-terminal A motif) or Myo1p-H/1/2 (*myo1Δ3A* lacking the C-terminal TH3 domain and A motif) (Figure S4C). However, Cdc15p-mEGFP failed to concentrate in patches of cells lacking Myo1p or depending on Myo1p without tail domains TH2, TH3 and A (*myo1Δ23A*) (Figure 3G), forming only a few spots that did not change in fluorescence intensity over time (Figure S4D).

While full-length Cdc15p-mEGFP persisted in patches for 8-12 s, small numbers of Cdc15p-mGFP lacking the single C-terminal SH3 domain (Cdc15pΔSH3-mEGFP) accumulated in patches for only ~3 s (Figure S4E) in spite of being expressed at a wild type level from the endogenous promoter (Figure S4B). This behavior confirmed that the SH3 domain is required to concentrate Cdc15p in actin patches but not contractile rings [39]. Fic1p interacts with the SH3 domain of Cdc15p, colocalizes with Cdc15p during interphase and in mitosis, and copurifies with clathrin heavy chain, a component of the actin patch [39]. Further work will be required to understand the role of Fic1p in clathrin-mediated endocytosis and its contribution to the function of Cdc15p.

Discussion

Localization and deletion of all seven F-BAR proteins and detailed analysis of two of these proteins suggest that each F-BAR protein has a distinct function in yeast cells, even along the pathway of clathrin-mediated endocytosis [24-30, 39]. Remarkably, one F-BAR protein, Cdc15p, has distinct roles in both endocytosis and cytokinesis [33]. The functional specificity of these proteins depends on unique properties of their F-BAR domains, which have very diverse amino acid sequences beyond the conserved amino acids. For example, long stretches of amino acids unique to Cdc15p link the a-helices of the F-BAR domain. Spatial and temporal variations in the lipid composition of fission yeast plasma membrane may influence the distributions of Cdc15p, Rga7p and Rga8p to different parts of the cell during the cell cycle. Rga7p and Rga8p also include Rho GTPase Activating Protein

domains at their C-termini and are localized to the cell tips during interphase and equatorial region during cell division.

Steps in clathrin-mediated endocytosis

Endocytosis in fission and the budding yeasts shares many common features, some with parallels in animal cells. Both yeasts require actin polymerization to form tubular invaginations of plasma membrane against turgor pressure [9, 40]. Fluorescence microscopy of live budding and fission yeast cells [5, 36] and electron microscopy of budding yeast [9] provided enough quantitative information [41] to formulate and test a mathematical model of actin assembly and turnover at sites of endocytosis [42]. In both yeasts, endocytosis occurs in at least three steps [1-4] (Figure 4). We use the actin patch time scale of Sirotkin et al [41] with time zero defined as the time when actin patch components move away from the plasma membrane.

Cells initiate endocytosis more than a minute before time zero by concentrating F-BAR protein Syp1p (both yeasts) or FCHo1/2 (animals) locally in the plasma membrane [43-46]. The F-BAR domains of these proteins bind PIP_2 and demark the membrane for a new endocytic event. By time -30 s an early module of proteins, consisting of clathrin (Clc1p and Chc1p), an EH-domain containing protein Ede1p (in budding yeast) and adapter proteins Pan1p and End4p (Sla2p in budding yeast), assemble on shallow (<50 nm) invaginations of the plasma membrane [41, 43, 46] with the clathrin coat occupying about 30 nm at the tip of the invagination [9]. Syp1p and Ede1p disappear near the onset of actin polymerization [43, 44], while clathrin remains associated with the invaginating membrane.

During the second step beginning at time -11 s, nucleation promoting factors Wsp1p and Myo1p start to accumulate followed by F-BAR proteins Bzz1p and Cdc15p (Figure 1D). These four proteins promote assembly of actin filaments by Arp2/3 complex starting at time -6 s. We show that fission yeast require an F-BAR protein in addition to Arp2/3 complex and either Wsp1p or Myo1p [36] for actin polymerization, patch movement and uptake of FM4-64. The movement of patch components in budding yeast corresponds to invagination of a narrow tubule of plasma membrane into the cytoplasm [9]. Given the similarity of the process in the two fungi, we assume this applies to fission yeast. In budding yeast myosin-I contributes to patch movement both its motor activity and activation of Arp2/3 complex [19].

The numbers and locations of proteins associated with actin patches provide the basis to predict the structures formed by the F-BAR proteins. F-BAR domains bind to lipid bilayers and induce membrane tubulation or assemble helical structures around tubular membranes [47]. A membrane tubule 57 nm in diameter can accommodate 8 F-BAR dimers around its circumference, so the peak number of 80 Bzz1p molecules would wrap around the tubular invagination 5 times and occupy as little as 20 nm along the length of the tubule. Electron micrographs suggested that the F-BAR domains of Cdc15p might be as long as 30 nm [48], so the peak number of 130 molecules might wrap ~8 times around the membrane invagination. These two zones of F-BAR proteins are not resolved by confocal fluorescence microscopy early in the process, but starting at time zero the center of the diffraction-limited spot of Bzz1p starts to move up to 250 nm from the cluster of Cdc15p, which is left behind in its original location near the cell surface. Therefore we expect that a 30 nm cuff of Cdc15p forms and remains close to the base of the tubule, while the 20 nm cuff of Bzz1p moves with the clathrin-coated tip of the invaginating tubule (Figure 4). Assuming that these F-BAR domains decorate the membrane in a closely packed helical array, our molecule counts show that the F-BAR proteins concentrate a high density of SH3 domains on these membrane invaginations: ~45,000 SH3 domains/μm^2 at the tip (2 SH3 domains/Bzz1p molecule) and ~16,500 SH3 domains/μm^2 near the neck of the tubular invagination (1 SH3

domain from Cdc15p). The high density of Bzz1p SH3 domains is expected to activate Wsp1p, because dimers of WASp-VCA are much more effective in stimulating Arp2/3 complex than monomers [49, 50].

One surprise is that recruitment of the F-BAR proteins follows in time and depends on the nucleation promoting factors, because the F-BAR domains presumably associate with the membrane tubule and it is easier to envisage a layered structure forming outward from the membrane surface with the F-BAR proteins acting as adapters between the membrane and their partner the nucleation promoting factors. Further work is required to clarify this conundrum.

In addition to recruiting F-BAR proteins to sites of endocytosis NPFs may activate the F-BAR protein to tubulate membranes. Structural studies showed that the SH3 domain of the full length F-BAR protein syndapin inhibits the potent membrane deforming activity, and that ligand binding to the SH3 domain unclamps the protein leading to membrane deformation [51, 52]. Thus SH3 domains of F-BAR proteins may serve both inhibitory as well as targeting roles [53].

Role of F-BAR proteins in *S. pombe* endocytic vesicle scission

The endocytic vesicle separates from the plasma membrane during the third step. In animal cells scission of the vesicle depends on dynamin and occurs just before dissociation of the clathrin coat [54]. Actin patch movements, vesicle scission and endocytosis in fungi are compromised in the absence of Wsp1p, Myo1p, Cdc15p or Bzz1p, so this step depends on the contributions of each of these proteins to actin polymerization [40]. The time of scission has not been documented in fungi, but we suggest that it occurs at about time +6 s when clathrin and coronin move beyond Wsp1p and Vrp1p, which stop moving about 300 - 400 nm from the cell surface. In cells lacking either Bzz1p or Cdc15p patches marked with coronin either move only short distances from the cell surface or retract back to the cell surface, so we suggest that vesicles loaded with the cargo fail to pinch off at this step and remain associated with the plasma membrane as a consequence of this lack of movement. Clathrin disassociates when it moves about 500 nm from the plasma membrane [5, 41], while coronin moves up to 800 nm into the cytoplasm.

Our observations provide clues regarding the roles of F-BAR proteins in actin polymerization associated with endocytosis and suggest a possible mechanism of vesicle scission (Figure 4). Since Bzz1p and Wsp1p separate from Cdc15p and Myo1p after time zero, actin polymerization driven by these nucleation promoting factors should concentrate actin filament formation in two zones along the invaginated membrane tubule. A ring of Cdc15p and Myo1p might stimulate one zone of actin assembly near the cell surface. A ring of activated Wsp1p would concentrate actin filament formation in a second zone near the tip of the invaginated membrane tubule. We suggest that the movement of Bzz1p and Wsp1p with most other patch proteins corresponds to the elongation of tubular invagination of the plasma membrane.

We propose that the two rings of F-BAR proteins and their partner nucleation promoting factors produce two opposing zones of actin polymerization that push against each other to elongate the tubular invagination of the plasma membrane, which breaks to release the coated vesicle (Figure 4). The high density of branched filaments arising in these two zones should preclude their interpenetration, allowing polymerization to produce force to stretch the membrane and contribute to scission of the vesicle without requiring precise orientation of the filaments relative to the membrane.

This new idea complements previous proposals to explain the vesicle scission. The 'mechanochemical' model [55] focuses on the contributions of the membrane lipids and the actin cytoskeleton. BAR domain proteins are proposed to bind and protect from hydrolysis PIP_2 in the tubular invagination of the plasma membrane. Hydrolysis of PIP_2 elsewhere along the tubular invagination generates PIP. The mobility of PIP and immobility of BAR domain proteins bound to PIP_2 produces a lipid phase separation that changes the membrane tension along the boundary between the two phases [55, 56]. The change in membrane tension coupled to the pulling and pushing forces of actin cytoskeleton and myosin I at the plasma membrane generate vesicle scission. An alternative model [57] based on in vitro reconstitution experiments proposes that BAR domain proteins mediate assembly of actin filaments at an angle to the invaginating membrane providing a pushing force that squeezes the membrane tubule and facilitates fission of the vesicle. The localization of over expressed Las17 (budding yeast WASp) on the invaginating membrane [58] is consistent with this hypothesis. Much more information about the organization of the molecules in actin patches is required to evaluate all of these hypotheses.

The overall pathway of endocytic patch assembly is similar in budding and fission yeast, but subtle differences include the total lifetime of the patches and the numbers of some patch proteins. Actin patches in *S. cerevisiae* depend on Bzz1p to activate the Wsp1p homolog Las17p [59], but appear lack a second F-BAR protein. However, type I myosin Myo5p, localizes with actin filaments to a different part of the plasma membrane invaginations than Bzz1p and Las17p [9], so two zones of actin polymerization may also contribute to endocytosis in budding yeast.

Experimental Procedures

Strain construction, growth conditions, and cellular methods

Supplemental Table I lists the *S. pombe* strains used in this study. We generated all strains by PCR-based gene targeting [60, 61] and standard genetic methods [62]. FM4-64 assay for endocytosis was performed as described previously. We stained cells with BODIPY 488-phalloidin (Invitrogen) [63].

Microscopy and data analysis

Fluorescence images of live cells were acquired with an Olympus IX-71 microscope with a 100×, 1.4 NA Plan Apo lens (Olympus) and an UltraView RS (PerkinElmer) or CSU-X1 (Andor Technology) confocal spinning disk confocal system equipped with an ORCA-ER CCD camera (Hamamatsu Corporation) or iXON-EMCCD camera (Andor Technology). Cells were imaged on 25% gelatin in EMM5S at 25°C. Patches were tracked using custom Image J plugins on images corrected for uneven illumination and camera noise. Fluorescence intensities of patches and the Mean square displacements of patches over time were calculated from the sum-projected 2D images. See Supplemental Experimental Procedures for detailed information on image acquisition and data analysis.

Bacterial expression constructs and protein purification

S. pombe proteins Arp2/3 complex, Myo1pTH2-SH3-CA, Wsp1p poly (p)-VCA (proline-rich domain, verprolin homology motif, connecting motif and acidic motif, nucleotides 385–1725); Bzz1pSH3SH3 (nucleotides 1561-1929); Bzz1pSH3 (nucleotides 1757-1929); and Cdc15pSH3 (nucleotides 2607-2784) were used in our biochemical experiments. For details on the cloning and purification of these proteins see Supplemental Experimental Procedures.

Quantitative pull-down assays

Equilibrium dissociation constants (K_d) were measured by quantitative pull-down assays [64]. We used KaleidaGraph (Synergy Software) to fit a binding isotherm to the dependence of the fraction of ligand bound [LR]/[L_{tot}] to [L_{tot}] using the equation [LR]/[L_{tot}] = (([R] + [L_{tot}] + K_d) − (([R] + [L_{tot}]+K_d) ^2 − 4* [R]* [L]) ^0.5)/2* [L_{tot}].

Actin polymerization assays

The time course of actin polymerization was measured by fluorescence of pyrene-labeled actin in 10 mM imidazole, 1 mM $MgCl_2$, 1 mM EGTA, 50 mM KCl [65]. Polymerization rates were measured from the time courses of actin polymerization when half of actin was polymerized. We measured the concentration of ends from the rate of elongation by using the following relationship: $R = k_+(A)(ends) - k_-(ends)$, where R is the rate of elongation, k_+ is the association rate constant (11.6 $\mu M^{-1}s^{-1}$), k_- is the dissociation rate constant (1.4 s^{-1}), A is the concentration of actin monomer and *ends* is the concentration of growing filament ends [66, 67].

Supplementary Material

Refer to Web version on PubMed Central for supplementary material.

Acknowledgments

We are grateful to Kathleen L. Gould (Vanderbilt University School of Medicine) and Vladimir Sirotkin (Upstate Medical University) for yeast strains. We thank Julien Berro, Vladimir Sirotkin and Chad McCormick for help with image analysis and valuable advice. We thank Irene Reynolds-Tebbs and Tara Reisbig for help with patch tracking. This work was supported by NIH research grants GM-026132 and GM-026338.

References

1. Kaksonen M, Toret C, Drubin D. Harnessing actin dynamics for clathrin-mediated endocytosis. Nat Rev Mol Cell Biol. 2006; 7:404–414. [PubMed: 16723976]
2. Conner S, Schmid S. Regulated portals of entry into the cell. Nature. 2003; 422:37–44. [PubMed: 12621426]
3. Doherty G, McMahon H. Mechanisms of endocytosis. Annu Rev Biochem. 2009; 78:857–902. [PubMed: 19317650]
4. Galletta B, Cooper J. Actin and endocytosis: mechanisms and phylogeny. Curr Opin Cell Biol. 2009; 21:20–27. [PubMed: 19186047]
5. Kaksonen M, Toret C, Drubin D. A modular design for the clathrin- and actin-mediated endocytosis machinery. Cell. 2005; 123:305–320. [PubMed: 16239147]
6. Itoh T, Erdmann K, Roux A, Habermann B, Werner H, De Camilli P. Dynamin and the actin cytoskeleton cooperatively regulate plasma membrane invagination by BAR and F-BAR proteins. Dev Cell. 2005; 9:791–804. [PubMed: 16326391]
7. Yu X, Cai M. The yeast dynamin-related GTPase Vps1p functions in the organization of the actin cytoskeleton via interaction with Sla1p. J Cell Sci. 2004; 117:3839–3853. [PubMed: 15265985]
8. Nannapaneni S, Wang D, Jain S, Schroeder B, Highfill C, Reustle L, Pittsley D, Maysent A, Moulder S, McDowell R, et al. The yeast dynamin-like protein Vps1:vps1 mutations perturb the internalization and the motility of endocytic vesicles and endosomes via disorganization of the actin cytoskeleton. Eur J Cell Biol. 2010; 89:499–508. [PubMed: 20189679]
9. Idrissi F, Grötsch H, Fernández-Golbano I, Presciatto-Baschong C, Riezman H, Geli M. Distinct acto/myosin-I structures associate with endocytic profiles at the plasma membrane. J Cell Biol. 2008; 180:1219–1232. [PubMed: 18347067]
10. Röthlisberger S, Jourdain I, Johnson C, Takegawa K, Hyams J. The dynamin-related protein Vps1 regulates vacuole fission, fusion and tubulation in the fission yeast, Schizosaccharomyces pombe. Fungal Genet Biol. 2009; 46:927–935. [PubMed: 19643199]

11. Pelkmans L, Püntener D, Helenius A. Local actin polymerization and dynamin recruitment in SV40-induced internalization of caveolae. Science. 2002; 296:535–539. [PubMed: 11964480]
12. Yarar D, Waterman-Storer C, Schmid S. A dynamic actin cytoskeleton functions at multiple stages of clathrin-mediated endocytosis. Mol Biol Cell. 2005; 16:964–975. [PubMed: 15601897]
13. Merrifield C, Perrais D, Zenisek D. Coupling between clathrin-coated-pit invagination, cortactin recruitment, and membrane scission observed in live cells. Cell. 2005; 121:593–606. [PubMed: 15907472]
14. Merrifield C, Feldman M, Wan L, Almers W. Imaging actin and dynamin recruitment during invagination of single clathrin-coated pits. Nat Cell Biol. 2002; 4:691–698. [PubMed: 12198492]
15. Swanson J, Watts C. Macropinocytosis. Trends Cell Biol. 1995; 5:424–428. [PubMed: 14732047]
16. Saffarian S, Cocucci E, Kirchhausen T. Distinct dynamics of endocytic clathrin-coated pits and coated plaques. PLoS Biol. 2009; 7:e1000191. [PubMed: 19809571]
17. Kaksonen M, Sun Y, Drubin DG. A pathway for association of receptors, adaptors, and actin during endocytic internalization. Cell. 2003; 115:475–487. [PubMed: 14622601]
18. Merrifield CJ, Feldman ME, Wan L, Almers W. Imaging actin and dynamin recruitment during invagination of single clathrin-coated pits. Nat Cell Biol. 2002; 4:691–698. [PubMed: 12198492]
19. Sun Y, Martin AC, Drubin DG. Endocytic internalization in budding yeast requires coordinated actin nucleation and myosin motor activity. Dev Cell. 2006; 11:33–46. [PubMed: 16824951]
20. Newpher TM, Smith RP, Lemmon V, Lemmon SK. In vivo dynamics of clathrin and its adaptor-dependent recruitment to the actin-based endocytic machinery in yeast. Dev Cell. 2005; 9:87–98. [PubMed: 15992543]
21. Engqvist-Goldstein A, Kessels M, Chopra V, Hayden M, Drubin D. An actin-binding protein of the Sla2/Huntingtin interacting protein 1 family is a novel component of clathrin-coated pits and vesicles. J Cell Biol. 1999; 147:1503–1518. [PubMed: 10613908]
22. Tsujita K, Suetsugu S, Sasaki N, Furutani M, Oikawa T, Takenawa T. Coordination between the actin cytoskeleton and membrane deformation by a novel membrane tubulation domain of PCH proteins is involved in endocytosis. J Cell Biol. 2006; 172:269–279. [PubMed: 16418535]
23. Yarar D, Waterman-Storer C, Schmid S. SNX9 couples actin assembly to phosphoinositide signals and is required for membrane remodeling during endocytosis. Dev Cell. 2007; 13:43–56. [PubMed: 17609109]
24. Fankhauser C, Reymond A, Cerutti L, Utzig S, Hofmann K, Simanis V. The S. pombe cdc15 gene is a key element in the reorganization of F-actin at mitosis. Cell. 1995; 82:435–444. [PubMed: 7634333]
25. Low C, Shui G, Liew L, Buttner S, Madeo F, Dawes I, Wenk M, Yang H. Caspase-dependent and -independent lipotoxic cell-death pathways in fission yeast. J Cell Sci. 2008; 121:2671–2684. [PubMed: 18653539]
26. Demeter J, Sazer S. imp2, a new component of the actin ring in the fission yeast Schizosaccharomyces pombe. J Cell Biol. 1998; 143:415–427. [PubMed: 9786952]
27. Nakano K, Mutoh T, Mabuchi I. Characterization of GTPase-activating proteins for the function of the Rho-family small GTPases in the fission yeast Schizosaccharomyces pombe. Genes Cells. 2001; 6:1031–1042. [PubMed: 11737264]
28. Soto T, Villar-Tajadura M, Madrid M, Vicente J, Gacto M, Pérez P, Cansado J. Rga4 modulates the activity of the fission yeast cell integrity MAPK pathway by acting as a Rho2 GTPase-activating protein. J Biol Chem. 2010; 285:11516–11525. [PubMed: 20164182]
29. Villar-Tajadura M, Coll P, Madrid M, Cansado J, Santos B, Pérez P. Rga2 is a Rho2 GAP that regulates morphogenesis and cell integrity in S. pombe. Mol Microbiol. 2008; 70:867–881. [PubMed: 18793338]
30. Yang P, Qyang Y, Bartholomeusz G, Zhou X, Marcus S. The novel Rho GTPase-activating protein family protein, Rga8, provides a potential link between Cdc42/p21-activated kinase and Rho signaling pathways in the fission yeast, Schizosaccharomyces pombe. J Biol Chem. 2003; 278:48821–48830. [PubMed: 14506270]
31. Soulard A, Lechler T, Spiridonov V, Shevchenko A, Li R, Winsor B. Saccharomyces cerevisiae Bzz1p is implicated with type I myosins in actin patch polarization and is able to recruit actin-polymerizing machinery in vitro. Mol Cell Biol. 2002; 22:7889–7906. [PubMed: 12391157]

32. Wu J, Kuhn J, Kovar D, Pollard T. Spatial and temporal pathway for assembly and constriction of the contractile ring in fission yeast cytokinesis. Dev Cell. 2003; 5:723–734. [PubMed: 14602073]
33. Carnahan R, Gould K. The PCH family protein, Cdc15p, recruits two F-actin nucleation pathways to coordinate cytokinetic actin ring formation in Schizosaccharomyces pombe. J Cell Biol. 2003; 162:851–862. [PubMed: 12939254]
34. Wu J, Pollard T. Counting cytokinesis proteins globally and locally in fission yeast. Science. 2005; 310:310–314. [PubMed: 16224022]
35. Wu J, McCormick C, Pollard T. Chapter 9: Counting proteins in living cells by quantitative fluorescence microscopy with internal standards. Methods Cell Biol. 2008; 89:253–273. [PubMed: 19118678]
36. Sirotkin V, Beltzner C, Marchand J, Pollard T. Interactions of WASp, myosin-I, and verprolin with Arp2/3 complex during actin patch assembly in fission yeast. J Cell Biol. 2005; 170:637–648. [PubMed: 16087707]
37. Lee W, Bezanilla M, Pollard T. Fission yeast myosin-I, Myo1p, stimulates actin assembly by Arp2/3 complex and shares functions with WASp. J Cell Biol. 2000; 151:789–800. [PubMed: 11076964]
38. Wu J, Sirotkin V, Kovar D, Lord M, Beltzner C, Kuhn J, Pollard T. Assembly of the cytokinetic contractile ring from a broad band of nodes in fission yeast. J Cell Biol. 2006; 174:391–402. [PubMed: 16864655]
39. Roberts-Galbraith R, Chen J, Wang J, Gould K. The SH3 domains of two PCH family members cooperate in assembly of the Schizosaccharomyces pombe contractile ring. J Cell Biol. 2009; 184:113–127. [PubMed: 19139265]
40. Aghamohammadzadeh S, Ayscough K. Differential requirements for actin during yeast and mammalian endocytosis. Nat Cell Biol. 2009; 11:1039–1042. [PubMed: 19597484]
41. Sirotkin V, Berro J, Macmillan K, Zhao L, Pollard T. Quantitative analysis of the mechanism of endocytic actin patch assembly and disassembly in fission yeast. Mol Biol Cell. 2010; 21:2894–2904. [PubMed: 20587778]
42. Berro J, Sirotkin V, Pollard T. Mathematical modeling of endocytic actin patch kinetics in fission yeast: disassembly requires release of actin filament fragments. Mol Biol Cell. 2010; 21:2905–2915. [PubMed: 20587776]
43. Stimpson H, Toret C, Cheng A, Pauly B, Drubin D. Early-arriving Syp1p and Ede1p function in endocytic site placement and formation in budding yeast. Mol Biol Cell. 2009; 20:4640–4651. [PubMed: 19776351]
44. Boettner D, D′Agostino J, Torres O, Daugherty-Clarke K, Uygur A, Reider A, Wendland B, Lemmon S, Goode B. The F-BAR protein Syp1 negatively regulates WASp-Arp2/3 complex activity during endocytic patch formation. Curr Biol. 2009; 19:1979–1987. [PubMed: 19962315]
45. Reider A, Barker S, Mishra S, Im Y, Maldonado-Báez L, Hurley J, Traub L, Wendland B. Syp1 is a conserved endocytic adaptor that contains domains involved in cargo selection and membrane tubulation. EMBO J. 2009; 28:3103–3116. [PubMed: 19713939]
46. Henne W, Boucrot E, Meinecke M, Evergren E, Vallis Y, Mittal R, McMahon H. FCHo proteins are nucleators of clathrin-mediated endocytosis. Science. 2010; 328:1281–1284. [PubMed: 20448150]
47. Frost A, Perera R, Roux A, Spasov K, Destaing O, Egelman E, De Camilli P, Unger V. Structural basis of membrane invagination by F-BAR domains. Cell. 2008; 132:807–817. [PubMed: 18329367]
48. Roberts-Galbraith R, Ohi M, Ballif B, Chen J, McLeod I, McDonald W, Gygi S, Yates Jr, Gould K. Dephosphorylation of F-BAR protein Cdc15 modulates its conformation and stimulates its scaffolding activity at the cell division site. Mol Cell. 2010; 39:86–99. [PubMed: 20603077]
49. Higgs H, Blanchoin L, Pollard T. Influence of the C terminus of Wiskott-Aldrich syndrome protein (WASp) and the Arp2/3 complex on actin polymerization. Biochemistry. 1999; 38:15212–15222. [PubMed: 10563804]
50. Padrick S, Cheng H, Ismail A, Panchal S, Doolittle L, Kim S, Skehan B, Umetani J, Brautigam C, Leong J, et al. Hierarchical regulation of WASP/WAVE proteins. Mol Cell. 2008; 32:426–438. [PubMed: 18995840]

51. Rao Y, Ma Q, Vahedi-Faridi A, Sundborger A, Pechstein A, Puchkov D, Luo L, Shupliakov O, Saenger W, Haucke V. Molecular basis for SH3 domain regulation of F-BAR-mediated membrane deformation. Proc Natl Acad Sci U S A. 2010; 107:8213–8218. [PubMed: 20404169]
52. Wang Q, Navarro MV, Peng G, Molinelli E, Goh SL, Judson BL, Rajashankar KR, Sondermann H. Molecular mechanism of membrane constriction and tubulation mediated by the F-BAR protein Pacsin/Syndapin. Proc Natl Acad Sci U S A. 2009; 106:12700–12705. [PubMed: 19549836]
53. Kumar V, Fricke R, Bhar D, Reddy-Alla S, Krishnan KS, Bogdan S, Ramaswami M. Syndapin promotes formation of a postsynaptic membrane system in Drosophila. Mol Biol Cell. 2009; 20:2254–2264. [PubMed: 19244343]
54. Taylor MJ, Perrais D, Merrifield CJ. A high precision survey of the molecular dynamics of Mammalian clathrin-mediated endocytosis. PLoS Biol. 2011; 9:e1000604. [PubMed: 21445324]
55. Liu J, Sun Y, Drubin DG, Oster GF. The mechanochemistry of endocytosis. PLoS Biol. 2009; 7:e1000204. [PubMed: 19787029]
56. Liu J, Kaksonen M, Drubin D, Oster G. Endocytic vesicle scission by lipid phase boundary forces. Proc Natl Acad Sci U S A. 2006; 103:10277–10282. [PubMed: 16801551]
57. Suetsugu S. The direction of actin polymerization for vesicle fission suggested from membranes tubulated by the EFC/F-BAR domain protein FBP17. FEBS Lett. 2009; 583:3401–3404. [PubMed: 19835875]
58. Galletta BJ, Chuang DY, Cooper JA. Distinct roles for Arp2/3 regulators in actin assembly and endocytosis. PLoS Biol. 2008; 6:e1. [PubMed: 18177206]
59. Soulard A, Friant S, Fitterer C, Orange C, Kaneva G, Mirey G, Winsor B. The WASP/Las17p-interacting protein Bzz1p functions with Myo5p in an early stage of endocytosis. Protoplasma. 2005; 226:89–101. [PubMed: 16231105]
60. Bähler J, Wu J, Longtine M, Shah N, McKenzie Ar, Steever A, Wach A, Philippsen P, Pringle J. Heterologous modules for efficient and versatile PCR-based gene targeting in Schizosaccharomyces pombe. Yeast. 1998; 14:943–951. [PubMed: 9717240]
61. Bahler J, Wu JQ, Longtine MS, Shah NG, McKenzie A 3rd, Steever AB, Wach A, Philippsen P, Pringle JR. Heterologous modules for efficient and versatile PCR-based gene targeting in Schizosaccharomyces pombe. Yeast. 1998; 14:943–951. [PubMed: 9717240]
62. Moreno S, Klar A, Nurse P. Molecular genetic analysis of fission yeast Schizosaccharomyces pombe. Methods Enzymol. 1991; 194:795–823. [PubMed: 2005825]
63. Arai R, Nakano K, Mabuchi I. Subcellular localization and possible function of actin, tropomyosin and actin-related protein 3 (Arp3) in the fission yeast Schizosaccharomyces pombe. Eur J Cell Biol. 1998; 76:288–295. [PubMed: 9765059]
64. Lee W, Ostap E, Zot H, Pollard T. Organization and ligand binding properties of the tail of Acanthamoeba myosin-IA. Identification of an actin-binding site in the basic (tail homology-1) domain. J Biol Chem. 1999; 274:35159–35171. [PubMed: 10574999]
65. Cooper J, Walker S, Pollard T. Pyrene actin: documentation of the validity of a sensitive assay for actin polymerization. J Muscle Res Cell Motil. 1983; 4:253–262. [PubMed: 6863518]
66. Pollard T. Measurement of rate constants for actin filament elongation in solution. Anal Biochem. 1983; 134:406–412. [PubMed: 6650826]
67. Machesky L, Mullins R, Higgs H, Kaiser D, Blanchoin L, May R, Hall M, Pollard T. Scar, a WASp-related protein, activates nucleation of actin filaments by the Arp2/3 complex. Proc Natl Acad Sci U S A. 1999; 96:3739–3744. [PubMed: 10097107]

Highlights

- F-BAR proteins Cdc15p and Bzz1p interact with different Arp2/3 complex activators
- During clathrin-mediated endocytosis Cdc15p and Bzz1p localize to 2 distinct zones
- Cells lacking either Cdc15p or Bzz1p assemble 3- to 5- fold less actin in patches
- Growth of two separate actin filament networks may contribute to membrane scission

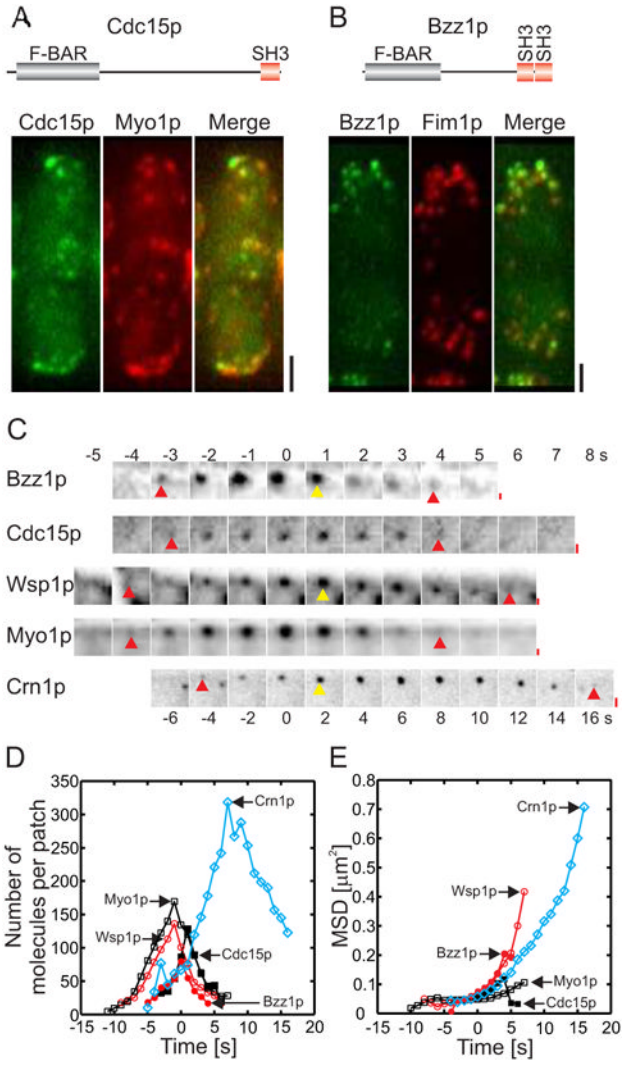

Figure 1. Quantitative analysis of actin patch dynamics

(A and B) Domain organization and localization of Cdc15p and Bzz1p in actin patches in live cells. Images are projections of 3D reconstructions. (A) Interphase cell expressing (left panel, green) mYFP-Cdc15p and (middle panel, red) mCFP-Myo1p. (Right panel) Merged image shows Cdc15p overlaps with Myo1p in many but not all actin patches because they represent different points in time. (B) Interphase cell expressing (left panel, green) Bzz1p-mEGFP and (middle panel, red) an actin binding protein fimbrin, Fim1p-mCherry. (Right panel) Merged image shows that Bzz1p overlaps with Fim1p in many but not all actin patches. Scale bar, 2 μm. (C) Montage of fluorescent micrographs (negative contrast images) of the time courses of Bzz1p-mEGFP, mEGFP-Cdc15p, mEGFP-Wsp1p, mEGFP-Myo1p and Crn1p-mEGFP accumulation and loss in actin patches. Regions of 12 ×12 pixels with an actin patch are shown at 1 s intervals for all proteins except for Crn1p-mEGFP, which is shown at 2 s intervals. Red arrows show the frame where the protein appeared and the last frame before it disappeared. Yellow arrows mark the frame where the patch started to move. Scale bar, 0.1 μm. (D) Time courses of the accumulation and loss of 5 actin patch proteins. Time zero seconds marks the initiation of patch movement. Symbols: (o, n = 20) Wsp1p; (□, n = 18) Myo1p; (■, n = 20) Cdc15p; (●, n=15) Bzz1p; and (◊, n = 30) Crn1p. (E) Time course of the mean square displacement of actin patches marked with (o, n = 20) Wsp1p, (□, n=18) Myo1p, (■, n = 20) Cdc15p, (●, n = 15) Bzz1p and (◊, n = 30) Crn1p.

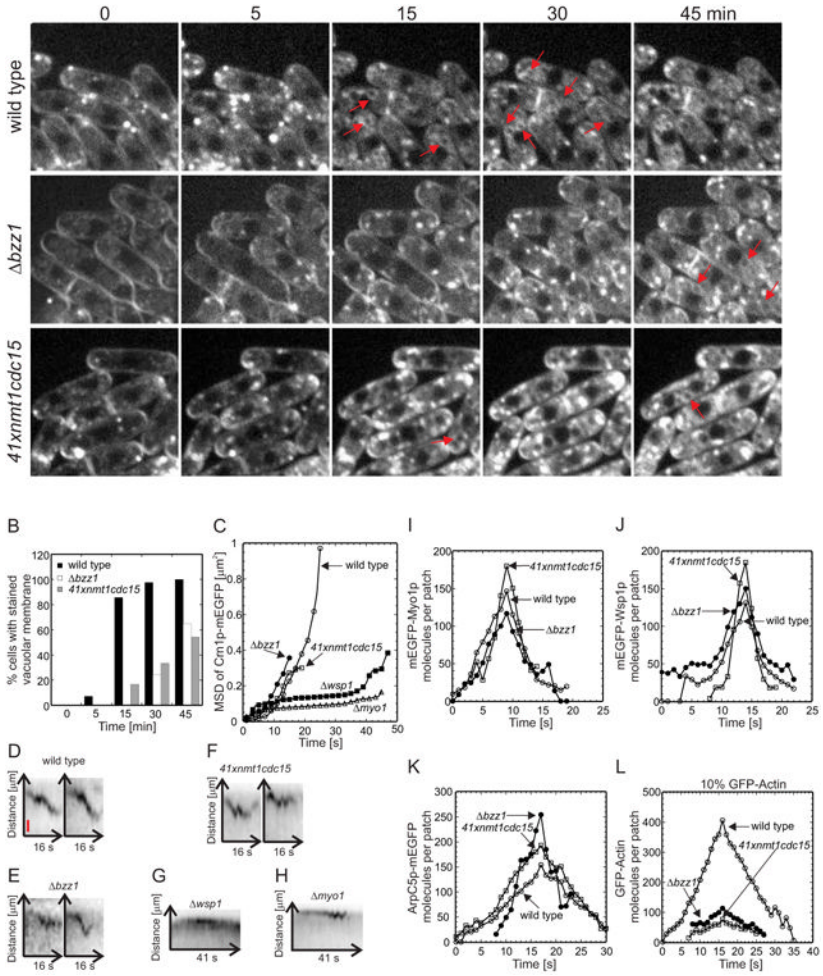

Figure 2. Effects of Bzz1p deletion or Cdc15p depletion on endocytosis and accumulation and loss of Myo1p, Wsp1p, Arp2/3 complex and actin, in actin patches

(A) Uptake of the fluorescent dye FM4-64 by endocytosis. Wild type, *Δbzzl and 41xnmt1cdc15* cells were incubated on ice for 15 min to block endocytosis, exposed to 20 μM FM4-64 in YE5S at 4° C for 15 min and shifted to 25° C to restart endocytosis. The images are single optical sections through the middle of the cells at different time points. Red arrows mark fluorescent vacuolar membranes. The rows show (top) wild type cells, (middle) *Δbzz1* cells and (bottom) *41xnmt1cdc15* cells depleted of Cdc15p. Scale bar 5 μm. (B) Quantitative analysis of endocytosis by scoring cells in time lapse movies that concentrated FM4-64 dye in the vacuolar membranes: (black bars) wild type cells (n= 42), (white bars) *Δbzz1* cells (n= 39) and (grey bars) *41xnmt1cdc15* cells (n=24). (C - H) Movements of actin patches tagged with coronin Crn1p-mEGFP in wild type and mutant cells. (C) Mean square displacement (MSD) of the diffraction-limited spot of Crn1p-mEGFP fluorescence over time. Symbols: (o, n = 10) wild type cells; (•, n = 12) *Δbzz1* cells lacking Bzz1p; (□, n = 13) *41xnmt1cdc15* cells depleted of Cdc15p; (■, n = 12) *Δwsp1* cells lacking Wsp1p; and (Δ, n = 11) *Δmyo1* cells lacking Myo1p. (D - H) Kymographs of individual Crn1p-mEGFP patches from five confocal sections imaged at 1 s intervals. A 24 × 14 pixel box was sum projected into a 24 × 1-pixel vertical lane and 16 lanes (D - F) or 41 lanes (G - H) were combined horizontally to generate negative contrast kymographs. (D) Wild type cells, (E) *Δbzz1* cells, (F) *41xnmt1cdc15* cells, (G) *Δwsp1* cells and (H) *Δmyo1* cells. Vertical red bar is 100 nm. (I - L) Time courses of the accumulation and loss of actin patch

proteins at 25°C in (○) wild type cells, (•) *Δbzz1* strains lacking Bzz1p and (□) *41xnmt1cdc15* cells depleted of Cdc15p. (I) mEGFP-Myo1p was expressed from the native locus and the numbers of molecules per patch were tracked over time in wild type cells (n = 21 patches), *41xnmt1cdc15* cells (n = 15) and Δ*bzz1* cells (n = 12). (J) mEGFP-Wsp1p was expressed from the native locus and the numbers of molecules per patch were tracked over time in wild type cells (n = 12 patches), *41xnmt1cdc15* cells (n = 23) and *Δbzz1* cells (n = 18). (K) The Arp2/3 complex subunit ArpC5p-mEGFP was expressed from the native locus and the numbers of molecules per patch were tracked over time in wild type cells (n = 12), *41xnmt1cdc15* cells (n = 7) and *Δbzz1* cells (n = 8). (L) GFP-actin was expressed from the *leu*$^{+}$ locus in the presence of wild type levels of native actin from a 41× nmt1 promoter in (○) wild-type cells, (•) Δ*bzz1* cells lacking Bzz1p and (□) from a 3× nmt1 promoter in *41xnmt1cdc15* cells. The numbers of molecules per patch were tracked over time.

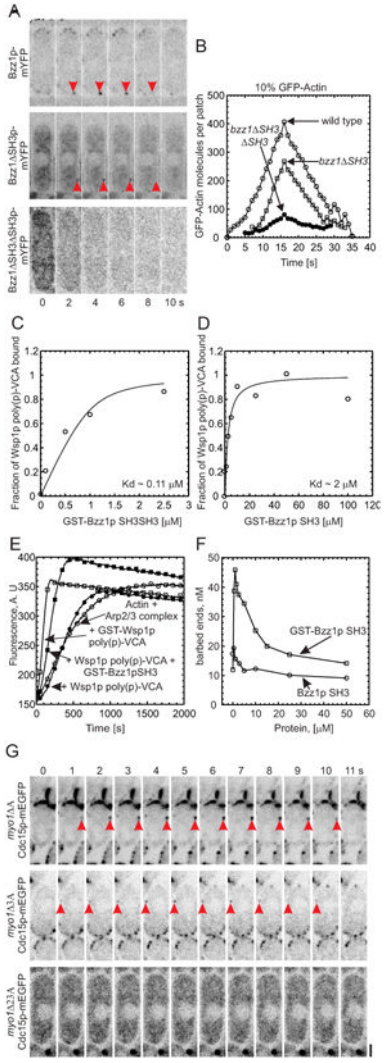

Figure 3. Interactions between F-BAR proteins and nucleation promoting factors in actin polymerization in actin patches

(A) Influence of Bzz1p SH3 domains on accumulation of the protein in actin patches. Time series of negative contrast fluorescence micrographs of single confocal sections at 2 s intervals: (upper row) Bzz1p-mYFP; (middle row) Bzz1pΔSH3-mYFP; and (lower row) Bzz1pΔSH3ΔSH3-mYFP cells. (B) Influence of Bzz1p SH3 domains on accumulation of GFP-actin in actin patches. GFP-actin was expressed from a 41×nmt1 promoter from the *leu*$^{+}$ locus in (○) wild type cells, (□) *bzz1*Δ*SH3* cells lacking the C-terminal SH3 domain or (•) *bzz1*Δ*SH3*Δ*SH3* cells lacking both the SH3 domains. The numbers of molecules per patch were tracked over time. (C, D) Equilibrium binding of Bzz1p SH3 domains to Wsp1p-poly (p)-VCA. Conditions: soluble 1 μM Wsp1p poly (p)-VCA was incubated with a range of concentrations of glutathione beads with bound (C) GST-Bzz1pSH3SH3 (residues 521-642) or (D) GST-Bzz1pSH3 (residues 586-642) at room temperature in 25 mM Tris - HCl pH 7.4, 75 mM NaCl, 1 mM EDTA, 1 mM DTT. Beads were pelleted at 16,000 × g and the bound fraction was calculated from concentration of Wsp1p poly (p)-VCA in the supernatant quantified by SDS-PAGE, staining with Coomassie Blue and densitometry. Equilibrium dissociation constants (Kd) were determined by fitting data to binding isotherms (solid lines). (E-F) Effects of Bzz1p SH3 domains on the nucleation promoting activity of Wsp1p. Time course of the polymerization of actin measured by the fluorescence

of pyrenyl-actin. Conditions: all samples contained 4 μM actin (10% pyrenyl-actin) and 50 nM *S. pombe* Arp2/3 complex in KMEI buffer. (E) Dependence on nucleation promoting factors: (○) no additions; (•) 500 nM Wsp1p-poly (p)-VCA; (□) 500 nM GST-Wsp1p-poly (p)-VCA; (■) 500 nM Wsp1p-poly (p)-VCA and 1 μM GST-Bzz1pSH3. (F) Dependence of the numbers of actin filament barbed ends created by 4 μM actin (10% pyrenyl-actin), 50 nM Arp2/3 complex and 500 nM Wsp1p-poly (p)-VCA on the concentration of (□) GST-Bzz1pSH3 or (○) Bzz1pSH3. (G) Dependence of Cdc15p-mEGFP targeting to actin patches on tail domains of Myo1p. Time series of negative contrast fluorescence micrographs at 1 s intervals of single confocal planes through cells depending on Cdc15p-mEGFP and with Myo1p lacking domains: (upper panel) *myo1ΔA* lacking the acidic motif; (middle panel) *myo1Δ3A* lacking tail homology domain 3 and acidic motif; and (lower panel) *myo1Δ23A* lacking tail homology domains 2 and 3 and the acidic motif. Red arrowheads indicate Cdc15p-mEGFP in patches. Scale bar 1 μm.

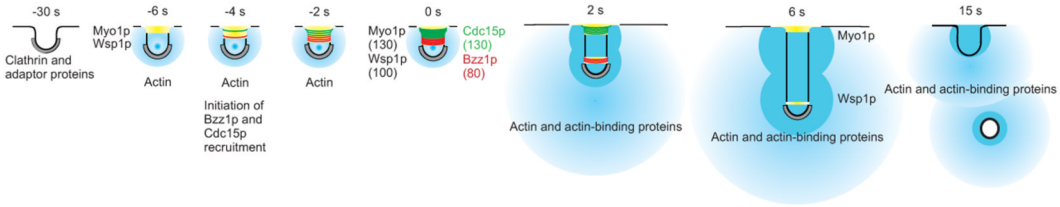

Figure 4. Hypothesis for the contributions of F-BAR proteins Cdc15p and Bzz1p to endocytosis

Eight time points in the life of an actin patch with time zero defined as the onset of movement of patch proteins away from the plasma membrane. The plasma membrane is a black line, clathrin is grey, nucleation promoting factors Wsp1p and Myo1p are yellow, Cdc15p is green, Bzz1p is red, actin filaments are blue and numbers of molecules are in parentheses. Clathrin is recruited 2 min prior to invagination. Nucleation promoting factors are recruited beginning at -10 s and peak prior to patch movement at -2 s (Figures 1C, 1D and 1E). F-BAR proteins Cdc15p and Bzz1p begin to accumulate at -5 s and peak at the onset of patch movement (Figures 1C, 1D and 1E). Recruitment of Cdc15p requires Myo1p (Figure 3G) and both the proteins remain near the cell surface. Bzz1p binds and activates Wsp1p to stimulate the assembly of branched actin filaments by Arp2/3 complex (Figures 3C - 3F). We assume that movement of Bzz1p, Wsp1p and many other patch proteins is associated with elongation of the plasma membrane tubule. We propose that expansion of branched filaments from two distinct zones of NPFs pushes the tip of the invaginating tubule away from the cell surface (2 - 6 s) (Figure 1E) contributing to scission of the coated vesicle. Both F-BAR proteins dissociate from the invaginating tubule as the vesicle moves into the cytoplasm (Figure 1D).

Table I

S. pombe F-BAR proteins

Gene/ Protein	Localization		Deletion
	Interphase	Mitosis	Mutant
cdc15/ Cdc15p	Actin patches	Contractile ring	Non-viable
bzz1/ Bzz1p	Actin patches	Actin patches	Viable
imp2/ Imp2p	Cytoplasm	Contractile ring	Viable
syp1/ Syp1p	Membrane/Actin patches	Membrane/Actin patches	Viable
rga7/ Rga7p	Cell tips	Cell tips, contractile ring and septum	Viable
rga8/ Rga8p	Cell tips	Septum	Viable
rga9/ Rga9p	Cytoplasm	Cytoplasm	ND*

*ND, not determined

Table II

Interactions between mutations of the genes for F-BAR proteins Cdc15p and Bzz1p and deletions of the genes for the activators of the Arp2/3 complex Wsp1p and Myo1p.

Mutant	Growth at the indicated temperature			
	25°C	30°C	32°C	36°C
Δbzz1	+++	+++	+++	++
cdc15-127 (ts)	+++	++	+	-
Δmyo1	++	ND*	ND*	-
Δwsp1	++	ND*	ND*	-
Δmyo1Δwsp1	-	-	-	-
Δbzz1cdc15-127(ts)	-	-	-	-
Δbzz1Δmyo1	-	-	-	-
Δbzz1Δwsp1	+++	++	++	+
cdc15-127(ts)Δmyo1	+++	++	++	+
cdc15-127(ts)Δwsp1	+++	-	-	-

The *cdc15-127* strain has a temperature-sensitive mutation that impairs contractile ring and septum formation during mitosis and rearrangement of actin patches is aberrant at restrictive temperatures. Double mutants were made by genetic crosses. Mutant strains were grown on YE5S plates with Phloxin B over a range of temperatures. (+++) Growth with no or very few pink colonies, (++) growth with pink colonies, (+) growth with dark pink colonies and (-) no growth. Dissections of asci from the cross between *Δbzz1*and *Δmyo1, Δwsp1* and *Δmyo1* yielded no viable double mutants. The tetrads were either of Non Parental Ditype with only two viable spores or Tetratype with three viable spores. Both the *Δwsp1* and *Δmyo1* strains carried a complementing plasmid to assist in these crosses. * ND, not determined.